AM4090 Write Up

Alison Peard

January 2020

Contents

1 Introduction

1.1 Motivation

Modelling the dynamics of ecosystems and predicting the effects that changes in an environment will have on species' populations has a variety of applications. From an environmental standpoint, it is useful for informing conservation policy by finding optimal fishing quotas or establishing locations to set up protected areas (Lucey et al., 2017),(McClellan et al., 2014), or to inform industry decision-making (Bouman, 1992). It can also be used to predict ecological disasters such as pest-outbreaks (Rivers-Moore, Hughes and de Moor, 2008).

Phytoplankton is an especially interesting topic of study due to it's far-reaching influences. It is a significant primary producer and at the base of the aquatic food chain (Lindsey and Scott, 2010), so being able to predict the dynamics of phytoplankton populations will allow us to make predictions about entire aquatic ecosystems (Jäger et al., 2008). Phytoplankton blooms (red-tides) can lead to anaerobic conditions and dead zones (US EPA, n.d.) in the ocean or the release of toxins into the water (Lindsey and Scott, 2010) both which lead to the die-off of other marine life. Toxins released in harmful algal blooms (HABs) can also travel up the food-chain and affect human health (Bennett, Dolin and Blaser, 2015).

Additionally, there is some scientific research going into the use of phytoplankton in bio-fuels (Narwani et al., 2016),(Coons, 2018). All of this makes understanding the dynamics of phytoplankton populations especially topical and relevant and motivated it as the subject for this project.

1.2 Partial Differential Equations

1.3 The Equations

This project studies a model proposed by Jäger, Diehl and Emans, (2010), which consists of a set set of three coupled nonlinear partial differential equations and two differential equations that describe the dynamics of phytoplankton in a one-dimensional column of fresh water. For this model, the z-axis is inverted and

deeper depths correspond to greater z-values. The equations are as follows,

$$\frac{\partial A}{\partial t} = p(I,q)A - l_{bg}A - v\frac{\partial A}{\partial z} + d\frac{\partial^2 A}{\partial z^2} \tag{1}$$

$$\frac{\partial R_b}{\partial t} = \rho(q,R_d)A - l_{bg}Rb - v\frac{\partial R_b}{\partial z} + d\frac{\partial^2 R_b}{\partial z^2} \tag{2}$$

$$\frac{\partial R_d}{\partial t} = -\rho(q,R_d)A + l_{bg}Rb + d\frac{\partial^2 R_d}{\partial z^2} \tag{3}$$

$$I(z) = I_0 exp - \left(\int_0^z kAdz + k_{bg}z\right) \tag{4}$$

$$\frac{\partial R_s}{\partial t} = vR_b(z_{max}) - rR_s \tag{5}$$

With functions p and ρ,

$$p(I,q) = \mu_{max}\left(\frac{q-q_{min}}{q}\right)\frac{I}{h+I} \tag{6}$$

$$\rho(q,R_d) = \rho_{max}\left(\frac{q_{max}-q}{q_{max}-q_{min}}\right)\frac{R_d}{m+R_d} \tag{7}$$

and,

$$q = \frac{R_b}{A} \tag{8}$$

The partial differential equation $\frac{\partial A}{\partial t}$ (1) measures the rate of change of the biomass of phytoplankton over the column of water as time changes. The variable A is measured as the algal carbon density in the water ($mg\,C\,m^{-3}$). Similarly, R_b represents the concentration of nutrient particles in the water which are bound in the algae, measured in $mg\,P\,m^{-3}$ and R_d represents the concentration of dissolved nutrients in the water , measured in $mg\,P\,m^{-3}$. I is the light intensity ($\mu mol\,photons\,m^{-2}\,s^{-1}$)and R_s is the pool of nutrients which become sedimented at the floor of the water column, ($mg\,P\,m^{-2}$).

The term q is the algal nutrient quota $\frac{R_b}{A}$, which can crudely be described as how "well-fed" the algae is and is related to A via the specific algal production rate function, p (6). The production rate is an increasing, saturating function of q and light, I, and acts as the growth function of A.

The function (7) for ρ is the measure of the rate at which algae take-up dissolved nutrients from the water (the "feeding" rate), transforming them to bound nutrients, and is a function of the variables q and R_d (how available dissolved nutrients are in the water column). For R_d constant, this reaches a maximum at $q = q_{min}$ and is zero when $q = q_{max}$.

The equation (4) for $I(z)$ measures the light intensity at each depth and is dependent on the depth z and the cumulative sum of the amount of algae in the water above the current depth multiplied by the specific light attenuation constant of the algae k.

In equation (1), the biomass of phytoplankton at a certain depth, $A(z)$ will decrease with the drift term $\frac{\partial A}{\partial z}$ which has the sinking-velocity coefficient v ($m\,day^{-}1$), and proportional to the respiration-loss term l_{bg}. It will increase with the diffusion term $\frac{\partial A^2}{\partial^2 z}$ with turbulent-diffusion coefficient d ($m^2\,day^{-}1$), and proportional to the production function p.

The concentration of nutrients bound in the algae R_b behaves similarly to A in the water column, which makes sense as it is bound within the algae so must move with it. This concentration will increases faster for large values of ρ, which indicates that the algae is taking in dissolved nutrients from the water at a faster rate.

The concentration of dissolved nutrients R_d has no sinking/drift term as it is assumed that gravity has no significant effect when these nutrients are part of the water. Only diffusion affects the distribution of dissolved nutrients in the water column. As algae take up dissolved nutrients from the water R_d will decrease as R_b grows, which is evident from the negative ρ and positive $l_{bg}R_b$ terms in the$\frac{\partial R_d}{\partial t}$ equation.

Equation (5) represents the rate of change of R_s, the concentration of sedimented nutrients at the floor of the water column. Nutrients bound in the algae are mineralized in the sediment as they reach z_{max} so R_s increases at a rate $vR_{bz_{max}}$ as bound nutrients sink to the floor of the water column. These nutri-

ents then re-enter the water as dissolved nutrients at a rate rR_s.
(POSSIBLY TALK MORE ABOUT ρ AND p)

1.4 Model Assumptions

A number of assumptions were made for the model proposed by Jaeger. The model assumes that there is a single nutrient which limits the production of the algae and that the only other influencing factor is light intensity. It assumes that amount of nutrients in the system (including sedimented nutrients) will remain constant. It assumes that the algae in have no ability of self-propulsion and must rely on turbulence to be transported back into the euphotic zone, which is where production may occur.

1.5 Boundary Conditions

The boundary conditions provided in the paper by Jaeger et al. will be used for this project. These are given in table 1 below.

"The boundary conditions are set such that algal biomass and particulate

Variable	Surface	z_{max}	z_{max} (ii)
A	$vA(0) - dA'(0) = 0$	$A'(z_{max}) = 0$	$A'(z_{max}) = 0$
R_b	$vR_b(0) - dR_b'(0) = 0$	$R_b'(z_{max}) = 0$	$R_b'(z_{max}) = 0$
R_d	$R_d'(0) = 0$	$dR_d'(z_{max}) - vR_b(z_{max}) = 0$	$rR_s - dR_d'(z_{max}) = 0$
I	$I(0) = I_0$		

Table 1: Table boundary conditions (Jäger, Diehl and Emans, 2010)

nutrients neither leave nor enter the system at the surface (no flux at z=0) but sink out at the bottom of the water column (convective flux at z=zmax). The latter condition implies that the fluxes of particulate carbon and nutrients into the sediment are and vA(z max) and vR (z max), respectively"(Jaeger,2010).

The Robin boundary conditions for A indicate that the net flux $J_A = vA - dA'$ is zero at the surface of the water for phytoplankton, and hence also for bound nutrients.

Plankton and nutrients don't leave or enter the water when $z = 0$. (NOTE) In the appendix of Jaeger's paper this is given by Neumann boundary conditions for A and R_b. (??? SHOULDN'T IT BE DIRICHLET FOR ABSORBING BOUNDARY?).

The surface boundary condition for R_d indicate that the surface of the water acts as a reflecting boundary for dissolved nutrients. (NEED TO FIX THIS)

Variable	Value	Definition
A		algal carbon density ($mg\,C\,m^{-3}$)
R_b		Concentration of particulate nutrients bound in algae ($mg\,P\,m^{-3}$)
R_d		Concentration of dissolved nutrients ($mg\,P\,m^{-3}$)
I		Light intensity ($\mu mol\,photons\,m^{-2}\,s^{-1}$)
I_0	300	Light intensity at the surface ($\mu mol\,photons\,m^{-2}\,s^{-1}$)
d	0.01-1000	Turbulent-diffusion coefficient ($m^2\,day^{-1}$)
v	0.25	Algal sinking velocity ($m\,day^{-1}$)
l_{bg}	0.1	Specific algal maintenance respiration losses (day^{-1})
k	.0003	Specific light-attenuation coefficient of algal biomass ($m^2 mg\,C^{-1}$)
k_{bg}	0.4	Background light-attenuation coefficient (m^{-11})
μ_{max}	1.2	Maximum specific algal production rate (day^{-1})
q_{min}	0.004	Maximum algal nutrient quota ($mg\,P\,mg\,C^{-1}$)
q_{max}	0.04	Minimum algal nutrient quota ($mg\,P\,mg\,C^{-1}$)
h	120	Half-saturation constant of light-dependant algal production ($\mu mol\,photons\,m^{-2}\,s^{-1}$)
ρ_{max}	0.2	Maximum specific algal nutrient uptake rate ($mg\,P\,mg\,C^{-1}\,day^{-1}$)
m	1.5	Half-saturation constant of algal nutrient uptake ($mg\,P\,m^{-3}$)
r	.02	Specific mineralization rate of sedimented nutrients (day^{-1})

Table 2: Table of variables used (Jäger, Diehl and Emans, 2010)

1.6 Variables of Interest

The variables of most interest for this project are d, the amount of turbulence in the water, and I_0 the light intensity at the surface. As light is needed for algal growth, the majority of production will occur in the euphotic zone of the water column, where $I(z)$ is large. As the algae in this model do not have the

ability of self-propulsion and have a higher density than water they will sink out of this zone at a rate v, along with the nutrients that are bound to them. Only turbulence can transport them back into a depth where production can take place, otherwise they will build up at z_{max} where $I(z_{max})$ is usually very low and die out at a rate $l_{bg}A$ or else enter the sediment. This project aims to reproduce the results of Jaeger et al. in the water column depth-turbulence space and additionally look for bifurcations caused by changes in d and I_0

1.7 Stiffness

2 Method

2.1 Initial Approach

To find equilibrium solutions for the system the initial approach used set all partial time derivatives to zero and attempted to solve the new system of ordinary differential equations. This was attempted via the shooting method. By defining $A_2 = A', R_{b2} = R_b'$ and $R_{d2} = R_d'$ as new variables the system was reduced to the first-order system given below,

$$\begin{aligned}
A_1' &= A_2 \\
A_2' &= \frac{1}{d}\left(vA_2 - p(I,q)A_1 + l_{bg}A_1\right) \\
R_{b1}' &= R_{b2} \\
R_{b2}' &= \frac{1}{d}\left(vR_{b2} - \rho(q,R_{d1})A_1 + l_{bg}R_{b1}\right) \\
R_{d1}' &= R_{d2} \\
R_{d2}' &= \frac{1}{d}\left(\rho(q,R_{d1})A_1 - l_{bg}R_{b1}\right) \\
I' &= -(kA_1 + k_{bg}z)I
\end{aligned}$$

with boundary conditions,

$$\begin{aligned}
vA(0) - dA'(0) &= 0 & A'(z_{max}) &= 0 \\
vR_b(0) - dR_b'(0) &= 0 & R_b'(z_{max}) &= 0 \\
R_d'(0) &= 0 & dR_d'(z_{max}) - vR_b(z_{max}) &= 0 \\
I(0) &= I_0
\end{aligned}$$

(NOTE: RD BOUNDARY CONDITIONS-CHANGE?)

Taking the initial conditions for $A_1 = 300, R_{b1} = 2.2, R_d = 30$ and $I = 300$ as known, the remaining values for A_2, R_{b2} and R_{d2} were guessed and a fourth-order Runge-Kutta method was used to interpolate the initial value problem to z_{max}. The predicted values for A_2, R_{b2} and R_{d2} and $dR_{d2} - vR_{b1}$ would be compared to the given boundary conditions. The intention was to then treat this differences between predicted and given boundary conditions as an equation in A_2, R_{b2} and R_{d2} and solve for it's roots by the (multivariate) Newton-Rhapson method.

The values at z_{max} obtained via Runge-Kutta iteration displayed very high sensitivity to initial conditions, small changes could lead to the solution blowing up, and hence any shooting method implementations failed to converge. This suggested that the system may be a stiff system, so instead a finite difference method was used to calculate the solutions for subsequent time steps over a long period of time until the system began to settle into a stable, stationary distribution.

(INCLUDE SOME BLOW UP DIAGRAMS?)

2.2 Theory of Forward and Centered Difference Approximation

Talk about stability, order of convergence, step-size choice etc.

2.3 The Finite Difference Method

The finite difference method was used to obtain numerical approximations of the differential equations (1)-(4). The first-order time derivative was approximated by the forward Euler method and the first and second-order space derivatives were approximated by first and second-order central difference equations. This

yielded,

$$A_z^{t+\Delta t} = A_z^t + \Delta t \left(p(I_z^t, q_z^t) A_z^t - l_{bg} A_z^t - v \frac{A_{z+\Delta z}^t - A_{z-\Delta z}^t}{2\Delta z} + d \frac{A_{z+\Delta z}^t - 2A_z^t + A_{z-\Delta z}^t}{\Delta z^2} \right) \tag{9}$$

$$R_{bz}^{t+\Delta t} = R_{bz}^t + \Delta t \left(\rho(q_z^t, R_{dz}^t) A_z^t - l_{bg} R_{bz}^t - v \frac{R_{bz+\Delta z}^t - R_{bz-\Delta z}^t}{2\Delta z} + d \frac{R_{bz+\Delta z}^t - 2R_{bz}^t + R_{bz-\Delta z}^t}{\Delta z^2} \right) \tag{10}$$

$$R_{dz}^{t+\Delta t} = R_{dz}^t + \Delta t \left(-\rho(q_z^t, R_{dz}^t) A_z^t + l_{bg} R_{bz}^t + d \frac{R_{dz+\Delta z}^t - 2R_{dz}^t + R_{dz-\Delta z}^t}{\Delta z^2} \right) \tag{11}$$

$$R_s^{t+\Delta t} = R_s^t + \Delta t \left(v R_{bz_{max}}^t - r R_s^t \right) \tag{12}$$

The equation (4) for I is discretized by expressing $\int_0^z kAdz$ as $\sum_i kA(i)$ where $i = 0, \Delta z, 2\Delta z, ..., z$.

2.4 Discretizing Boundary Conditions

To discretize the boundary conditions the second-order formula for the first derivative (Sauer, 2012), $f'(x) = \frac{1}{2h}\left(-3f(x) + 4f(x+h) - f(x+2h)\right) + O(h^2)$ is used.

In the case of Neumann boundaries where f'(x) = 0,

$$\begin{aligned} -3f(0) + 4f(1) - f(2) &= 0 \\ -f(M-2) + 4f(M-1) - 3f(M) &= 0 \end{aligned}$$

Using this we obtain the discretized boundary conditions at the surface:

$$\begin{aligned} \frac{d}{2v\Delta z + 3d}\left(4A_1 - A_2\right) &= A_0 \\ \frac{d}{2v\Delta z + 3d}\left(4R_{b1} - R_{b2}\right) &= R_{b0} \\ \frac{1}{3}(4R_{d1} - R_{d2}) &= R_{d0} \\ I(0) &= I_0 \end{aligned}$$

and at zmax:

$$\frac{1}{3}(-A_{z-2} + 4A_{z-1}) = A_z$$
$$\frac{1}{3}(-R_{bz-2} + 4R_{bz-1}) = Rb_z$$
$$\frac{1}{3d}\left(4dR_{dz-1} - dR_{dz-2} + 2v\Delta z R_{bz}\right) = R_{dz}$$

or, (FIX THIS)

$$\frac{1}{3}(-A_{z-2} + 4A_{z-1}) = A_z$$
$$\frac{1}{3}(-R_{bz-2} + 4R_{bz-1}) = Rb_z$$
$$\frac{1}{3d}\left(4dR_{dz-1} - dR_{dz-2} + 2r\Delta z R_s\right) = R_{dz}$$

3 Building Up to a Solution

(INCLUDE PLOTS OF DRIFT-DIFFUSION ONLY ETC. AND TALK ABOUT EFFECTS OF ADDING EACH TERM).

4 Results

4.1 Reproducing the Depth-Turbulence Plots

The primary aim was to reproduce the heatmaps of the first two rows of figure 1 (shown below). The first row shows concentrations of phytoplankton at different depths z (y-axis), for different water column depths z_{max} (x-axis), for five different turbulence values (d). The second row shows the same for total nutrient concentration $R = R_d + R_b$.

As was done in the paper, the stationary value was calculated fifty times for each value of $d = 0.1, 1, 10$, increasing z_{max} in 1 metre increments each time. To speed up simulations, a spacial step size of $\Delta z = 0.1$ was used instead of $\Delta z = 0.02$ as in the paper. Resulting visuals for $d = 0.1$ were similar and satisfactory. For $d = 1.0$, however, the general shape was similar but the peak concentration of algae was located at a shallower depth in the water column than in figure 1 and there was less algae overall. The heatmap of nutrients was

more in keeping with the visuals but again, the distribution appeared shifted to a shallower depth. (INCLUDE 3D TIME-EVOLUTION PLOT HERE AND SEE IF POPULATION STILL INCREASING/DECREASING)

The results obtained for $d = 10$ were quite different to those shown in figure 1. The effect of turbulence appears much greater in figure 2 where there are almost homogeneous vertical distributions of both phytoplankton and nutrients. There are concentrations as high as $1200 mg\,C\,m^{-3}$ for A in figure 1 but concentrations do not exceed $500 mg\,C\,m^{-3}$ in figure 2. A 3-dimensional space-time plot (ADD THIS IN) indicate that the concentration of algae is decreasing with time for $d = 10$. This suggests that the finite difference approach used in this paper is more accurate for lower values of d and perhaps a smaller step size needs to be used for large values of d. (CHECK THIS BIT) (INCLUDE PLOTS

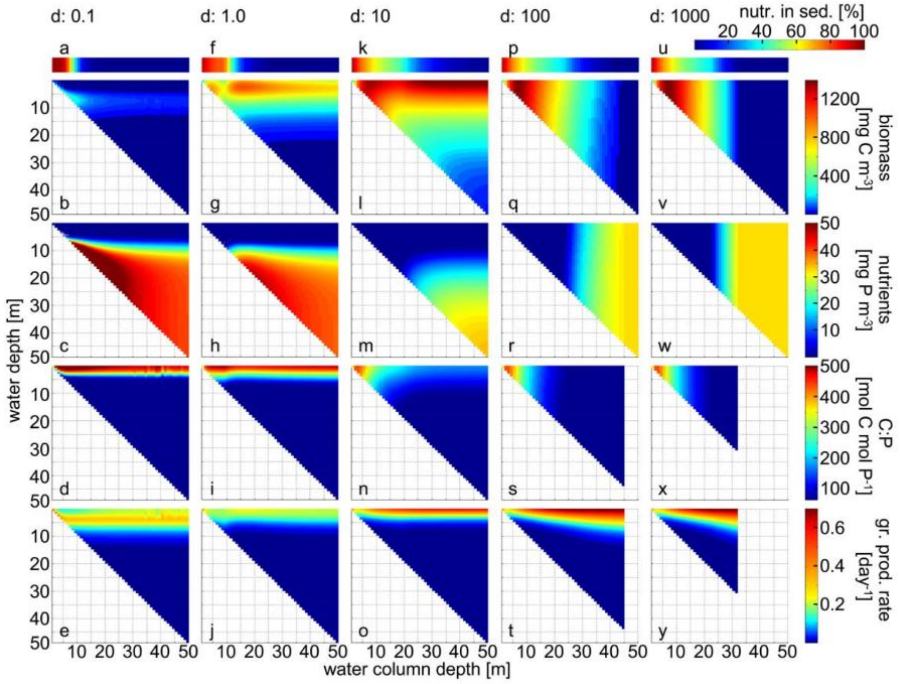

Figure 1: Depth-Turbulence Stationary Distributions (Jäger, Diehl and Emans, 2010)

OF PEAK CONCENTRATION LOCATION FOR LIKE IN THE PAPER TO COMPARE PROPERLY)

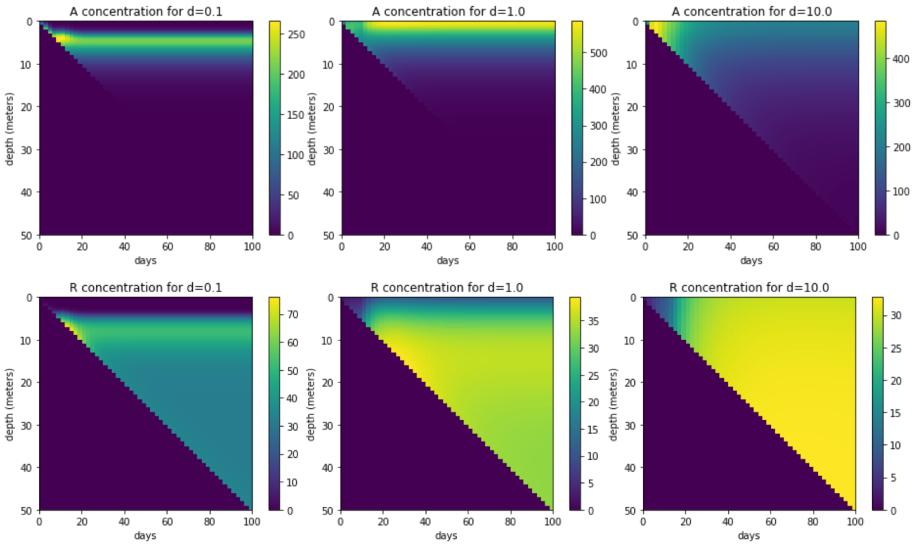

Figure 2: Depth-Turbulence Stationary Distributions by Finite Difference Method

4.2 Light Shifts

Doubling Light Intensity:

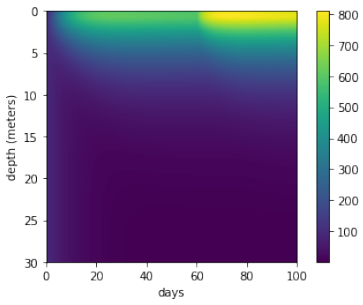

Figure 3: Heatmap

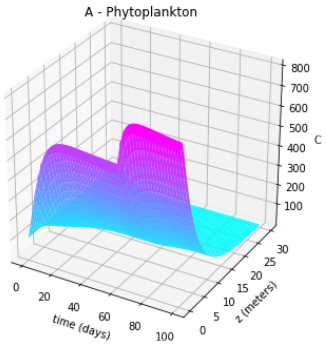

Figure 4: 3D Plot

Halving Light Intensity:

(Possibility of creating a function (sine-like) for I0 that changes throught a

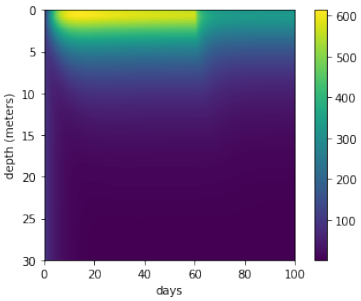

Figure 5: Heatmap

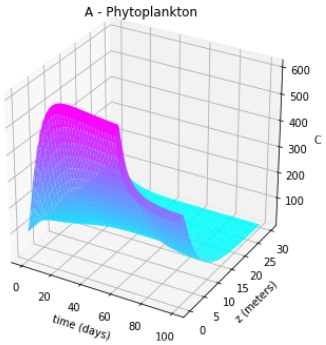

Figure 6: 3D Plot

day.)

4.3 Stationary Distributions for Various Turbulence Values

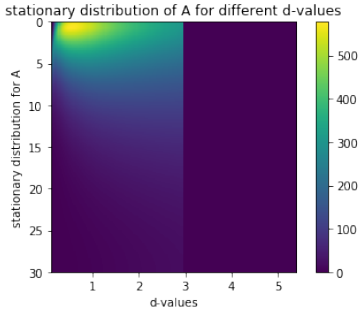

Figure 7: Heatmap

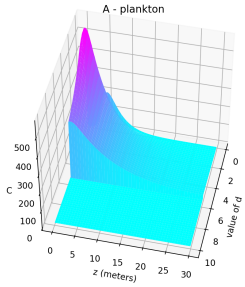

Figure 8: 3D Plot

Both figures 3 and 4 suggest the stationary distribution of A has decreasing concentration with increasing d.

5 Bibliography

Bennett, J., Dolin, R. and Blaser, M. (2015). Mandell, Douglas, and Bennett's principles and practice of infectious diseases. 8th ed. p.3192.

Bouman, B. (1992). Linking physical remote sensing models with crop growth simulation models, applied for sugar beet. International Journal of Remote Sensing, 13(14), pp.2565-2581.

Coons, R. (2018). Danish researchers look to harness bioluminescent algae to light cities — Nuu. [online] Biofuelsdigest.com. Available at: http://biofuelsdigest.com/nuudigest/2018/05/07/danish-researchers-look-to-harness-bioluminescent-a [Accessed 10 Jan. 2020].

Jäger, C., Diehl, S., Matauschek, C., Klausmeier, C. and Stibor, H. (2008). Transient Dynamics of Pelagic Producer-Grazer Systems in a Gradient of Nutrients and Mixing Depths. Ecology, 89(5), pp.1272-1286.

Jäger, C., Diehl, S. and Emans, M. (2010). Physical Determinants of Phytoplankton Production, Algal Stoichiometry, and Vertical Nutrient Fluxes. The American Naturalist, 175(4), pp.E91-E104.

Lindsey, R. and Scott, M. (2010). What are Phytoplankton?. [online] Earthobservatory.nasa.gov. Available at: https://earthobservatory.nasa.gov/features/Phytoplankton [Accessed 10 Jan. 2020].

Lucey, J., Palmer, G., Yeong, K., Edwards, D., Senior, M., Scriven, S., Reynolds, G. and Hill, J. (2017). Reframing the evidence base for policy-relevance to increase impact: a case study on forest fragmentation in the oil palm sector. Journal of Applied Ecology, 54(3), pp.731-736.

McClellan, C., Brereton, T., Dell'Amico, F., Johns, D., Cucknell, A., Patrick, S., Penrose, R., Ridoux, V., Solandt, J., Stephan, E., Votier, S., Williams, R. and Godley, B. (2014). Understanding the Distribution of Marine Megafauna in the English Channel Region: Identifying Key Habitats for Conservation within the Busiest Seaway on Earth. PLoS ONE, 9(2), p.e89720.

Narwani, A., Lashaway, A., Hietala, D., Savage, P. and Cardinale, B. (2016). Power of Plankton: Effects of Algal Biodiversity on Biocrude Production and

Stability. Environmental Science Technology, 50(23), pp.13142-13150.

Rivers-Moore, N., Hughes, D. and de Moor, F. (2008). A model to predict outbreak periods of the pest blackflySimulium chutteri Lewis (simuliidae, Diptera) in the Great Fish River, Eastern Cape province, South Africa. River Research and Applications, 24(2), pp.132-147.

Sauer, T. (2012). Numerical analysis. 2nd ed. Pearson Education, Inc., p.384.

US EPA. (n.d.). The Effects: Dead Zones and Harmful Algal Blooms — US EPA. [online] Available at: `https://www.epa.gov/nutrientpollution/effects-dead-zones-and-harmful-algal-blooms` [Accessed 10 Jan. 2020].